Effect of micro-channel technique on solar collector performance

IOP Conf. Series: Materials Science and Engineering **518** (2019) 032047 doi:10.1088/1757-899X/518/3/032047

Effect of micro-channel technique on solar collector performance

Jalal M. Jalil[1*], Nashwan A. Abdulkadhim[1]
[1]University of Technology, Electromechanical Engineering Department, Baghdad, Iraq
[*]Corresponding author e-mail: jalalmjalil@gmail.com

Abstract. The use of the micro-channel technique is available in many applications, but its applications in the solar collectors are very few, so this research makes a clear contribution in this field. The heat transfer to the flowing air is improved by using micro-channel technique. Numerical and experimental of the impact of micro-channel technique on solar air collector performance is investigated. Navier Stokes and energy equations is solved by using 3D forced convection laminar model inside rectangular micro-channels of absorber plate in solar air collector. The numerical calculations are extended to analyze the performance of a solar air collector by using micro-channel absorber plate. Experimentally, an absorber plate was manufactured from Aluminum metal with 30 rectangular micro-channels (length 0.9, width 0.004, height 0.0008 m) is constructed with measurements facilities of velocity, temperature, and differential pressure to achieve the experimental results. The tests are carried out indoor utilizing a solar simulator. Validation is achieved by using comparing the numerical results with experimental outcomes and a good agreement is executed among them, it is approximately (3-4%). Both factors air flow rate and solar irradiance have been studied as one of the essential factors in solar collectors. The numerical and experimental parameters studied are air flow of 0.0019, 0.0029, 0.0044 and 0.0053 kg/s and irradiance of 200, 400, 600 and 800 W/m^2. The performance was investigated by measuring outlet air temperature. The micro-channel absorber shows good performance, the maximum outlet air temperature reaches 72.5^{o}C.

1. Introduction

Solar air collector is a simple thermal system utilized for low-temperature heating. The properties of solar collectors are mainly based on absorption plate and its design, selective coating, thermal insulation, tilt angle, and working fluid, therefore, many researchers have tried to enhance the overall performance of collectors with various techniques by increasing the heat transfer between the absorption plate and the flowing air. The main advantage of the mini-channel/micro-channel which pulls researcher is its high heat transfer potential combining attributes of high surface area per volume, small working fluid and large heat transfer coefficient. micro-channel is a good technique, using the air as a working fluid, and utilized this technique in the solar air collector.

Gamrat et al. 2005 [1] demonstrated numerically the flowing fluid of both 3 and 2-dimensional in a rectangular micro-channels of convective heat transfer. Finally, the comparison between the measured and calculated temperature fields and solar irradiance is illustrated. Hetsroni et al. 2005 [2] Studied the ability of a conventional theory to foretell the hydrodynamic (D_h) property of laminar Newtonian incompressible outflow in micro-channels in the range of hydraulic diameter from D_h = 15 μm to 4 mm. They noted that no difference in behavior pattern of flow between micro-channels and macro-scale flow, at least down to 50 μm diameter. Al-Bakhit and Al-Fakhri 2006 [3] studied numerically a parallel flow in micro-channel heat exchanger to determine the effect of different

parameters on the accuracy and performance of heat transfer coefficient assumption which is constant. There is a great change in the total heat transfer coefficient in the developing region and the 3-dimensional heat transfer in the heat exchanger wall should be included in the analysis. Allen 2007 [4] studied experimentally and numerically the fluid circulation and heat moving inside the microchannel. The results showed through these types of large contract simulations using fresh information within the turbulent transition routine in addition to along with the theoretical links with respect to laminar. The guessing associated with the heat sink inside the microchannel gets along has been investigated by Sabbah et al. 2009 [5]. The results showed a significant increase in the heat transfer coefficient under certain conditions for heat flux rates of 100 W/cm2 and 500 W/cm2, DH =0.166mm, that is mainly depends on input temperature, channel outlet and melting temperature. Bertsch et al. 2009 [6] investigated the heat transfer of boiling flow of the two cooling system R-245fa or R-134a in a microchannel, cold are evaporators. The range of rectangular micro-channels of D_h 1.09, 0.54mm with countenance ratio 2.5 is considered. Due to the change with heat flow and vapor type, a Heat transfer coefficient is created. It has been proven that the essence of boiling is a heat transfer rule. Biswal et al. 2009 [7] are utilized a coolant flow inside the microchannel in order to study the generation of large heat (>100 W/cm2) and cooling electronic devices more efficiently. Comparing empirical and practical data, good results were observed. Hydrodynamics thermal flow in rectangular microchannel consist of a group of fifteen parallel rectangular channels of depth, width D_h (0.772 ± 0.005, 1.1 ± 0.02, 0.907 mm), sequentially is studied by Agarwal, et al. 2010 [8]. Accordingly, the study reveals that conventional theory, which predicts thermo-hydrodynamics of growing internal flows, is largely applicable for the microchannels. No new physical phenomenon or effect is observed. Mohammed and Shuaib 2011 [9] studied heat transfer characteristics in wavy micro-channel with a rectangular cross-section of a wavy field that vary from 125 to 500 μm was numerically scrupulous. Its miles observed that the heat transfer performance of the wavy micro-channels is lots better than the straight micro-channels with the same cross-section. The pressure drop is much smaller than achieving enhanced heat transfer of wavy micro-channels. Both the coefficient of friction and shear stress are increased proportionally with the amplitued of the wavy micro-channels increased. Thermal analysis of mini channel-based totally solar flat plate collector turned into supplied by using Mansour 2013 [10] in order to study a heat transfer characteristics and the pressure drop of working fluid. Comparing empirical and practical data, good results were observed. The proposed novel collector that has thermohydraulic performance was compared to that of the conventional flat-plate collector. The comparison found out that the heat removal factor of the novel collector is better than that of the conventional one by 16.1%. Mohamed and El-Baky 2013 [11] offered heat transfer experiments that performed via a mini-channel heat sink with different configurations. The results demonstrated that the heat transfer to air stream is increased with increasing both of air mass flow rate and channel base temperature. The rectangular channels have higher thermal performance than those in the triangles under the same conditions. Amraoui and Aliane 2014 [12] are compared theoretically and experimentally utilizing CFD device with respect to flow and temperature distribution inside the flat-plate solar collector. The aim of this work was to think of a virtual work and to test the specific work using a CFD device with respect to temperature and flow along the solar collector. The outlet temperature of the air was looked at with experimental outcomes and there was good agreement between them. Xia and Chan 2015 [13] explained that heat transfer was improved in micro channels. The area becomes larger as the input area becomes relatively smaller, so a new heat exchanger design is proposed based on these additional small impacts. Jiandong et al. 2015 [14] are numerically studied performance of the flat-plate collector by taking into account spacing of collector tube, thickness of absorber plate, tube diameter of collector, thickness of insulating layer and the length of collector tube. The numerical data are compared and analyzed with experimental ones. The results display that the instantaneous performance can significantly improve either by lowering the spacing of collector tube or increasing the thickness of absorber plate. Sun et al. 2016 [15] are based on a finite-difference approach in order to demonstrate a mathematical model under forced convection mode for the solar air collector (SAC). The temperature of the air outlet is in reasonable agreement with those obtained from theoretical and experimental studies. Al-Asadi, et al. 2016 [16] presented the effect of heat transfer in the micro-channel within a modern design (vortex generator (VGs)). VGs described here are shown to

offer significant potential in combating the challenges of heat transfer in the technological drive towards lower weight/smaller volume electrical and electronic devices. Abdulrasool et al. 2017 [17] studied the flow boiling heat transfer, a pressure drop in a copper multi-parallel micro-channels heat sink using R134a as a working fluid. The heat transfer coefficient increases with heat flux and system pressure but there is insignificant mass flux. They didn't found pressure effect at low mass flux while the heat transfer coefficient increased with pressure at the high mass flux values. Liu et al. 2017 [18] studied experimentally heat flow in the rectangular micro-channels of two-phase flow. It was found that the characteristics affect mainly of the phase distribution in the channels parallel of 2 phase flow, the inlet real velocity, length the gas slug inlet. The best distributions of the phase were obtained at the case of high speed with short slugs. Kwon et al. 2018 [19] investigated experimentally the results heat transfer of single-phase in a compact cross-flow micro-channel of heat exchanger, with air flowing via the heat exchanger in order to take of heat from a flow of closed loop of refrigerant R245fa. This work allows to understand the heat transfer in compact micro-channel devices and show a high-power-density of a micromachined metallic heat exchanger.

The solar air collector performance investigates with the effect of micro-channel technique throughout an outlet air temperature. Experimentally, the tests will carry out indoor using solar simulator consists of three tungsten halogen lamps. Most researchers nowadays prefer to use the so-called solar simulator to avoid the limited time of testing where it may not be available at this time specified the appropriate solar conditions, therefore most researchers are using a solar simulator to provide the exact conditions to be studied in the laboratory. Both factors air flow rate and solar irradiance will be studied as one of the essential factors in solar collectors, thereby when any amendment inside the solar collector, for example, the use of micro-channel technique should be studied these two factors. Changing the airflow to four values of 0.0019, 0.0029, 0.0044 and 0.0053 kg/sec with four values to irradiance of 200, 400, 600 and 800 W/m^2. An absorber plate with 30 rectangular micro-channels (length 0.9, width 0.004, height 0.0008 m). Validation of the code by using (FORTRAN 90) will perform. The numerical calculations will extend to analyze the overall performance within micro-channel technique in a solar collector.

2. Experimental apparatus and general behavior:

The experimental apparatus is photographically demonstrated in Figure 1. The experiment apparatus consists of the following:-

1) Main Test Section (solar collector).
2) A solar simulator (Tungsten halogen lamps).
3) A centrifugal fan (Blower).
4) Control valve.
5) Voltage regulator.
6) Temperature sensors (Thermocouples).
7) Measurement Devices:-
    a) Temperature Recorder 12 Channels (Temperature measurement).
    b) Digital manometer (Pressure measurement).
    c) Vane type thermo-anemometer (Measurement of air velocity).
    d) Solar Power Meter (Irradiance measurement).
    e) Voltmeter.
8) Arduino.
9) Battery (12 volts).
10) Personal computer using (Laptop).

One model of experiential has been manufactured locally for testing the thermal performance of micro-channel and used it in the solar air collector. In the experimental work, the micro-channels of solar air collector is supplied with fresh air. Temperature sensors (Thermocouples) read the temperature of absorber plate, inlet and outlet air. The inserted type thermocouples are installed at the surface of the absorber plate at 4 points and 2 sensors in the inlet and outlet air ducts that connected

with (Temperature Recorder 12 Channels) to measure the average temperature of the plate and the air temperature, as demonstrated in Figure 2. The air inlet temperature of micro-channels is the ambient room temperature and is fixed at 25° C. The inlet air velocity is controlled to investigate their effect on micro-channel to get air temperature exit as required. The pressure drop is measured across the duct by using digital manometer.

The heat transfer from the hot absorbent material plate to the air that flowing through channels is increased by using the micro-channel technique due to its small hydraulic diameter (D_h). This increment in heat transfer is usually accomplished with an additional pressure drop. There are 30 of micro-channels distributed on the base plate that has dimensions (90 cm of length, 15 cm of width and 0.6 cm of height) including 15 channels on the top surface and 15 channels on the bottom surface, and the distance between channels is 5 mm. It includes a standard set of 32 Aluminum fins, a design of rectangular type fins with a hydraulic diameter of 1.3 mm with the channel length, channel width and channel height 900 mm, 4 mm and 0.8 mm, respectively. The microchannel is covered with a piece similar in dimensions and it manufactured from an Aluminum alloy, the dimensions of covers is 90cm of length, 15cm of width and 0.2cm height in order to ensure minimum heat resistance, and the perfect thermal connection at the right micro-channel, as indicated in Figure 3. The tests are carried out indoor using solar simulator throughout this experiment that consists of three-tungsten halogen lamps. Most researchers nowadays prefer to use the so-called solar simulator to avoid the limited time of testing where it may not be available at this time specified the appropriate solar conditions, therefore most researchers are using a solar simulator to provide the exact conditions to be studied in the laboratory. The radiation intensity falls on the collector is measured by a solar power meter. Figure 4 shows photographs of absorber plate with micro-channels. The glass cover consists of glass windows with dimensions of 88cm length, 22cm of width and 0.3 cm of height. A gap is created between the glass cover and the absorbing surface with a thickness of 4 cm. The rectangular duct of plywood has an internal size of (90×24×10) cm^3.

3. Numerical analysis and a mathematical formulation

Steady-state 3D forced convection laminar model is used to solve Navier Stokes and energy equations of airflow inside rectangular micro-channel of solar air collector. Finite volume of (31×11×16) mesh nodes is used. The numerical calculations extended to analyze the overall performance within micro-channel technique in a solar collector. CFD is an important tool to analyze and type to prediction the temperature and velocity distribution in the flow of the microchannel and also to predict the temperature of the body of micro-channel.

3.1 Governing Equations: -

I-Continuity equation

$$\frac{\partial}{\partial x}(\rho u)+\frac{\partial}{\partial y}(\rho v)+\frac{\partial}{\partial z}(\rho w)=0 \qquad \dots(1)$$

II-Momentum Equations

X-direction (U-Momentum)

$$\frac{\partial}{\partial x}(uu)+\frac{\partial}{\partial y}(uv)+\frac{\partial}{\partial z}(uw)=-\frac{1}{\rho}\frac{dP}{dx}+\nu\left(\frac{\partial^2 u}{\partial x^2}+\frac{\partial^2 u}{\partial y^2}+\frac{\partial^2 u}{\partial z^2}\right) \qquad \dots(2)$$

Y-direction (V-Momentum)

$$\frac{\partial}{\partial x}(vu)+\frac{\partial}{\partial y}(vv)+\frac{\partial}{\partial z}(vw)=-\frac{1}{\rho}\frac{dP}{dy}+\nu\left(\frac{\partial^2 v}{\partial x^2}+\frac{\partial^2 v}{\partial y^2}+\frac{\partial^2 v}{\partial z^2}\right) \qquad \dots(3)$$

Z-direction (W-Momentum)

$$\frac{\partial}{\partial x}(uw)+\frac{\partial}{\partial y}(vw)+\frac{\partial}{\partial z}(ww)=-\frac{1}{\rho}\frac{dP}{dz}+\nu\left(\frac{\partial^2 w}{\partial x^2}+\frac{\partial^2 w}{\partial y^2}+\frac{\partial^2 w}{\partial z^2}\right) \qquad \dots(4)$$

III-Energy equation

$$\frac{\partial}{\partial x}(uT)+\frac{\partial}{\partial y}(vT)+\frac{\partial}{\partial z}(wT)=\frac{k}{\rho C_p}\left(\frac{\partial^2 T}{\partial x^2}+\frac{\partial^2 T}{\partial y^2}+\frac{\partial^2 T}{\partial z^2}\right) \quad \ldots(5)$$

3.2 The General Transport Equation:

The transportation equations of the momentum, energy, and continuity have the general form

$$\frac{\partial}{\partial x}(\rho u\emptyset)+\frac{\partial}{\partial y}(\rho v\emptyset)+\frac{\partial}{\partial z}(\rho w\emptyset)=\frac{\partial}{\partial x}\left(\Gamma_\emptyset\frac{\partial\emptyset}{\partial x}\right)+\frac{\partial}{\partial y}\left(\Gamma_\emptyset\frac{\partial\emptyset}{\partial y}\right)+\frac{\partial}{\partial z}\left(\Gamma_\emptyset\frac{\partial\emptyset}{\partial z}\right)+S_\emptyset \quad \ldots(6)$$

3.3 Thermal Analysis of Solid Walls

If the system is in a steady state, then the heat flow in the x, y and z directions may be calculated from the Fourier equation:

$$q=-kA\frac{\partial T}{\partial x} \quad \ldots(7)$$

3.3.1 Absorber Plate (upper plate)

When irradiance passes through the glass cover and barge into the surface of black painted plate surface with high absorptivity, the majority of the energy is ingested by the plate and transmitted to the flowing air in the micro-channel of a collector. The energy balance at any node of the upper plate represented as follows:

$$q_e+q_w+q_n+q_s+q_{conv(p2-af2)}+q_{conv(p2-g)}+q_{rad(p2-p1)}+q_{rad(p2-g)}+q_{flux}=0 \quad \ldots(8)$$

q_e, q_w, q_n *and* q_s are the heat transferred by conduction to the east, west, north, and south of the node respectively which can be given by

$$q_e=k_{ap}A_x\frac{dT}{dx}=\frac{k_{ap}A_x}{\Delta x}(T_{p2(i,j,k)}-T_{p2(i+1,j,k)}) \quad \ldots(9)$$

$$q_w=k_{ap}A_x\frac{dT}{dx}=\frac{k_{ap}A_x}{\Delta x}(T_{p2(i,j,k)}-T_{p2(i-1,j,k)}) \quad \ldots(10)$$

$$q_n=k_{ap}A_z\frac{dT}{dz}=\frac{k_{ap}A_z}{\Delta z}(T_{p2(i,j,k)}-T_{p2(i,j,k+1)}) \quad \ldots(11)$$

$$q_s=k_{ap}A_z\frac{dT}{dz}=\frac{k_{ap}A_z}{\Delta z}(T_{p2(i,j,k)}-T_{p2(i,j,k-1)}) \quad \ldots(12)$$

$q_{conv(p2-af2)}$is the heat transferred by convection from the upper plate to the flowing air in the upper channel which can be given by

$$q_{conv(p2-af2)}=h_{af}A_y dT=h_{af}A_y(T_{p2(i,j,k)}-T_{af2}) \quad \ldots(13)$$

$q_{conv(p2-g)}$is the heat transferred by convection from the upper plate to glass cover through air gap. It will be calculated using the term k_e (effective or apparent thermal conductivity).

$$q_{conv(p2-g)}=k_eA_y\frac{dT}{dy}=\frac{k_eA_y}{\delta}(T_{p2(i,j,k)}-T_{g(i,j,k)}) \quad \ldots(14)$$

$$\frac{k}{k_e}=0.212(Gr_\delta \mathrm{Pr})^{0.25} \quad \ldots(15)$$

$q_{rad(p2-g)}$ is the heat transferred by radiation from the upper plate to glass cover.

$$q_{rad(p2-g)}=h_{rad(p2-g)}A_y\left(T_{p2(i,j,k)}-T_{g(i,j,k)}\right) \quad \ldots(16)$$

$$h_{rad(p2-g)} = \frac{\sigma\left(T_{p2(i,j,k)}+T_{g(i,j,k)}\right)\left(\left(T_{p2(i,j,k)}\right)^2+\left(T_{g(i,j,k)}\right)^2\right)}{\left(1/\varepsilon_{p2}\right)+\left(1/\varepsilon_{g}\right)-1} \quad \ldots(17)$$

$q_{rad(p2-p1)}$is the heat transferred by radiation from upper plate to middle plate.

$$q_{rad(p2-p1)} = h_{rad(p2-p1)}A_y\left(T_{p2(i,j,k)} - T_{p1(i,j,k)}\right) \quad \ldots(18)$$

$$h_{rad(p2-p1)} = \frac{\sigma\left(T_{p2(i,j,k)}+T_{p1(i,j,k)}\right)\left(\left(T_{p2(i,j,k)}\right)^2+\left(T_{p1(i,j,k)}\right)^2\right)}{\left(1/\varepsilon_{p2}\right)+\left(1/\varepsilon_{p1}\right)-1} \quad \ldots(19)$$

q_{flux} is the solar radiation absorbed by absorber plate.

$$q_{flux} = (\tau_g\alpha_{ap})_{av}A_yG \quad \ldots(20)$$

Equation (8) can be expressed as:

$$\frac{k_{ap}A_x}{\Delta x}\left(T_{p2(i,j,k)} - T_{p2(i+1,j,k)}\right) + \frac{k_{ap}A_x}{\Delta x}\left(T_{p2(i,j,k)} - T_{p2(i-1,j,k)}\right) + \frac{k_{ap}A_z}{\Delta z}\left(T_{p2(i,j,k)} - T_{p2(i,j,k+1)}\right) + \frac{k_{ap}A_z}{\Delta z}\left(T_{p2(i,j,k)} - T_{p2(i,j,k-1)}\right) + h_{af}A_y\left(T_{p2(i,j,k)} - T_{af2}\right) + \frac{k_eA_y}{\delta}\left(T_{p2(i,j,k)} - T_{g(i,j,k)}\right) + h_{rad(p2-p1)}A_y\left(T_{p2(i,j,k)} - T_{p1(i,j,k)}\right) + h_{rad(p2-g)}A_y\left(T_{p2(i,j,k)} - T_{g(i,j,k)}\right) + (\tau_g\alpha_{ap})_{av}A_yG = 0 \quad \ldots(21)$$

Suppose:

$$C_e = C_w = \frac{k_{ap}A_x}{\Delta x}$$

$$C_n = C_s = \frac{k_{ap}A_z}{\Delta z}$$

$$C_{af} = h_{af}A_y$$

$$C_g = \frac{k_eA_y}{\delta} + h_{rad(p2-g)}A_y$$

$$C_{p1} = h_{rad(p2-p1)}A_y$$

$$C_j = C_e + C_w + C_n + C_s + C_{p1} + C_g + C_{af}$$

After substituting these terms in Eq. (21) the result is

$$T_{p2(i,j,k)}=\left[C_eT_{p2(i+1,j,k)} + C_wT_{p2(i-1,j,k)} + C_nT_{p2(i,j,k+1)} + C_sT_{p2(i,j,k-1)} + C_{af}T_{af} + C_gT_{g(i,j,k)} + C_{p1}T_{p1(i,j,k)} + (\tau_g\alpha_p)_{av}A_yG\right]/C_j \quad \ldots(22)$$

The temperature of any point on the upper plate can be calculated by Eq. (22)

3.4 Calculations of Heat Transfer

The hydraulic diameter and Reynolds number are calculated by

$$Dh = \frac{4\left(free\ area\right)}{wetted\ \ perimeter} = \frac{4*Wch*Hch}{2(Wch+Hch)}. \quad \ldots(23)$$

Reynolds number, *Re* is defined as,

$$\mathrm{Re} = \frac{\rho v d}{\mu} \quad \ldots(24)$$

In order to calculate the convective heat flux in a single-phase flow, one must monitor the mass flow rate and measure the difference of outlet and inlet temperatures of water contained in the cooling

system.

$$Q = m \cdot * C_p * (T_{aout} - T_{ain)} \quad \ldots(25)$$

The aforementioned equation will provide the basic tools for interpreting and better understanding the significance of the acquired data. Where the averaged heat transfer coefficients were defined as

$$h = \frac{Q}{A_s*(T_w - T\ )} \quad \ldots (26)$$

Where *As* = (2*H* + 2*W*) *L*. The channel wall temperature, *Tw*, is assumed to be uniform and equal to the average of the readings from the four thermocouples located on the test section. The average heat transfer coefficient is calculated as.

$$\text{Where } T \text{ (Average mean temperature)} = \frac{T_{in+T_{out}}}{2} \quad \ldots (27)$$

The corresponding average Nusselt number is defined as

$$N_u = \frac{h*D_h}{K} \quad \ldots (28)$$

Solar collector thermal efficiency can be calculated using

$$\eta_{th} = \frac{\dot{m}c_p(T_o - T_i)}{IA_c} \quad \ldots (29)$$

Thermohydraulic performance of solar air collector is evaluated on the basis of effective efficiency and is written as

$$\eta_{eff} = \frac{Q_u - P_m}{IA_c} \quad \ldots (30)$$

Where *Pm* is the mechanical energy required for air propelling through the duct which is given by

$$p_m = \frac{\dot{m}\Delta p}{\rho} \quad \ldots (31)$$

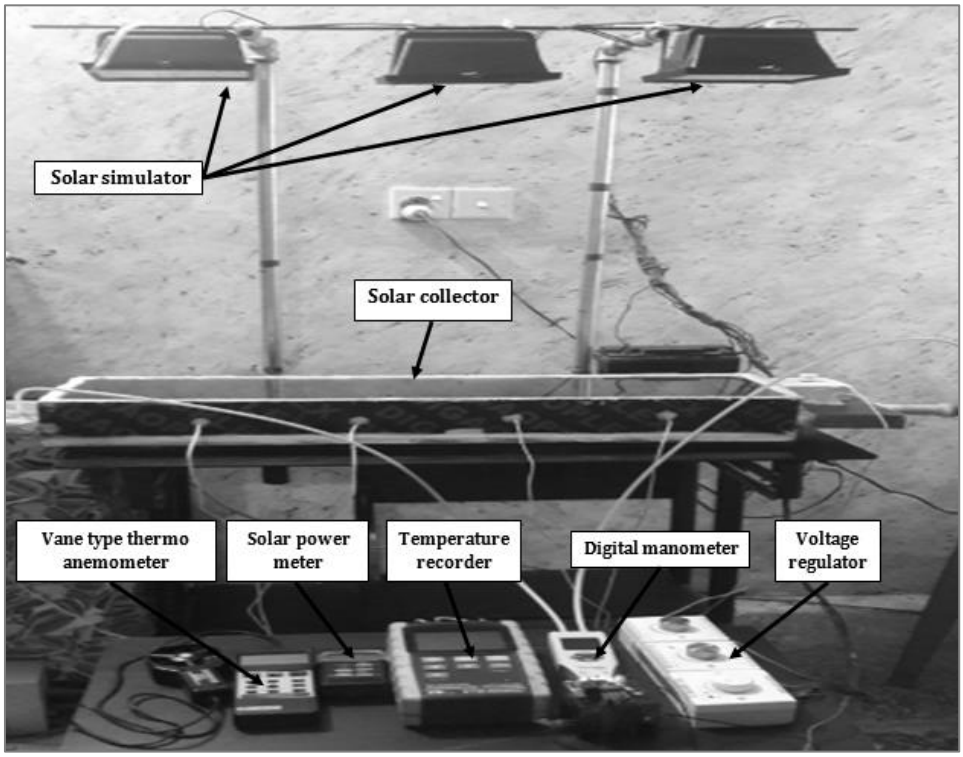

Figure 1. Photograph of the experimental apparatus

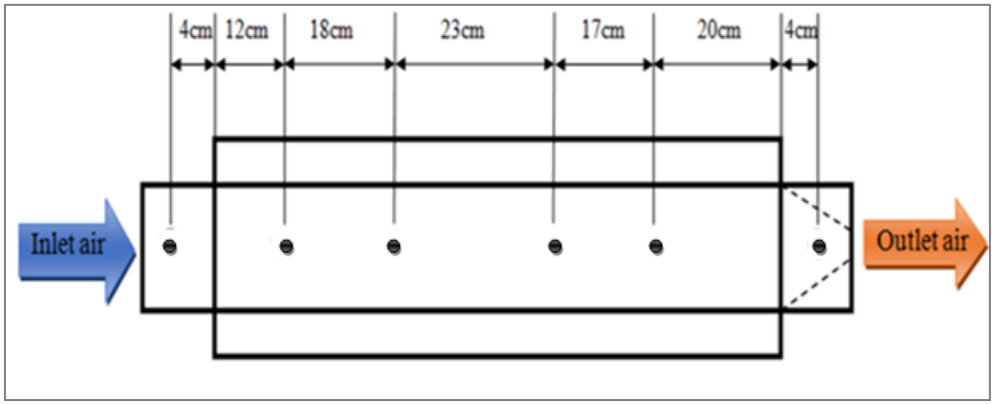

Figure 2. Thermal sensor distribution along an absorber plate

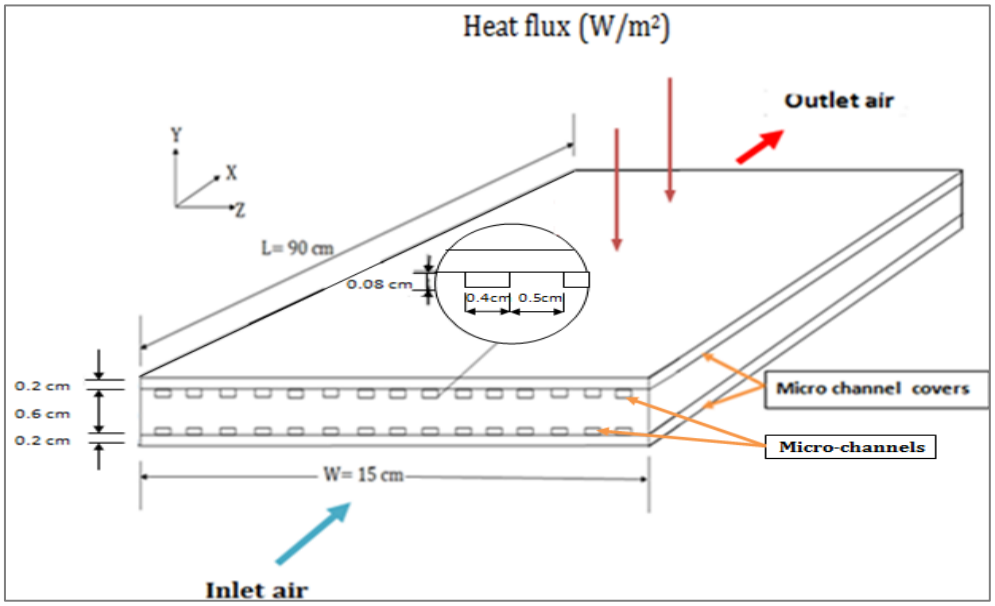

Figure 3. Sketch of micro-channels with its covers (Absorber plate)

Figure 4. Photograph of micro-channels

4. Result and discussion

We did not find research identical to my research and so we resorted to comparison with the closest research which is the finned solar air collector. It is actually different about the micro-channel but it is the closest research. The Comparison between the present work, finned and plane solar air collectors of Ref [20] at irradiance 800 W/m^2 for outlet air temperature is shown in Figure 5. It is shown that the highest outlet air temperature of the present work is 72.5° C, whereas at finned solar air collector is 68° C, and 46.5° C of plane solar air collector. The variation of absorber plate temperature with distance from air entrance at different values of irradiance at 0.0019 kg/s is illustrated in Figure 6. The

maximum temperature rise obtained of the absorber plate is 99.2° C at an airflow of 0.0019 kg/s (minimum air flow) and irradiance of 800 W/m^2. Figure 7 shows the variation of the air outlet temperature of the collector with air flow at different values of irradiance. It is shown that temperature decreases as the air flow increases from 0.0019 kg/s to 0.0053 kg/s. It is clear from the above Figure that increasing the amount of heat (irradiance), as well as a decrease in airflow cause an increase in the outlet air temperature. The experimental variation of the air temperature difference ΔT (°C) with air flow at different values of irradiance is shown in Figure 8. The heat transfer coefficient increases with increases of mass flux by increases in velocity, and increases of irradiance. The value of Nusselt number was low, due to the length of the collector is high. The results obtained at four values of irradiance 200, 400, 600 and 800 W/m² and range of air flow 0.0019, 0.0029, 0.0044 and 0.0053 kg/s. The curve trend refers to increases Nusselt number when the mass flow increases for the four working air flow, as well as increasing in solar irradiance. Figure 9 shows the variation of Nusselt number with irradiance at different values of air flow.

Figure 10 illustrates the experimental variation of thermal efficiency tested of solar air collector as a function of mass flow rates at different values of irradiance. It is found that the highest thermal efficiency is obtained by using a micro-channel technique which is 72.8%. The effect of hydraulic losses caused by the micro-channel on solar air collector efficiency in term of effective efficiency is represented in Figure 11, which is 70.44%. The highest advantage is at the highest value of flow rate in this study, it is clear that thermal and effective efficiency increase with increasing mass flow rate and decrease with increasing irradiance. Figure 12 shows isotherm contours of the plate at an irradiance of 800 W/m² and air flow of 0.0019 kg/s. It is observed that temperature begins to increase along the duct (flow direction), while in the radial direction, the high temperature at the channel walls begins to decline towards the center of the channel, Whereas in the radial direction of the absorber plate, the high temperature at bottom surface, due to an insulation effect begins to decline towards the upper surface of the plate. The flow field in micro-channel 2D, at an air flow of 0.0053 kg/s is illustrated in Figure 13. The velocity decreases in the direction towards the duct walls until it becomes zero at the walls, while it has a maximum value at the center of the channel.

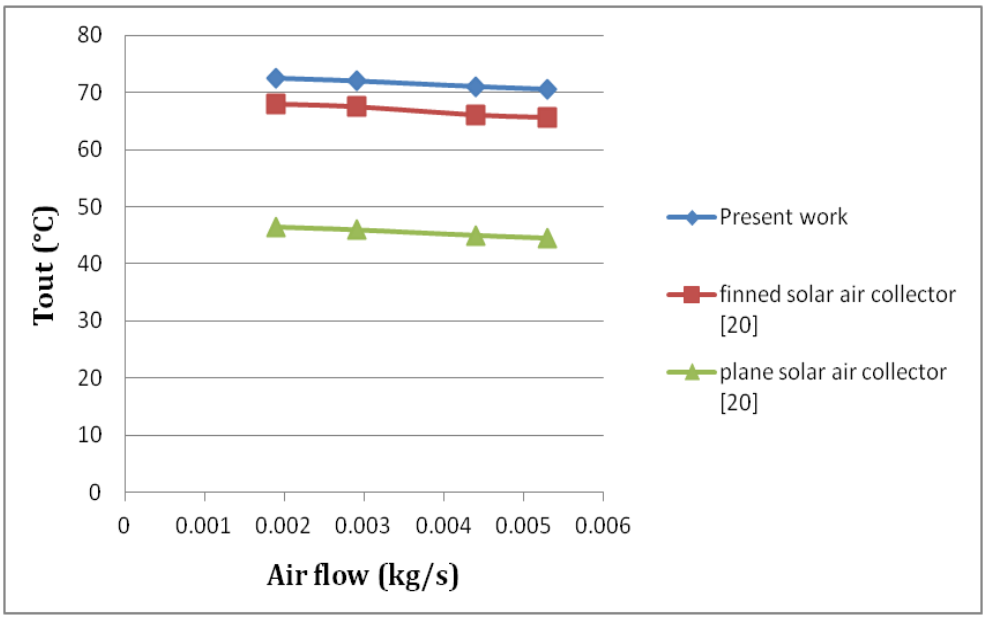

Figure 5. Comparison between present work with finned and plane solar air collectors of Ref [20] at irradiance 800 W/m^2 for outlet air temperature

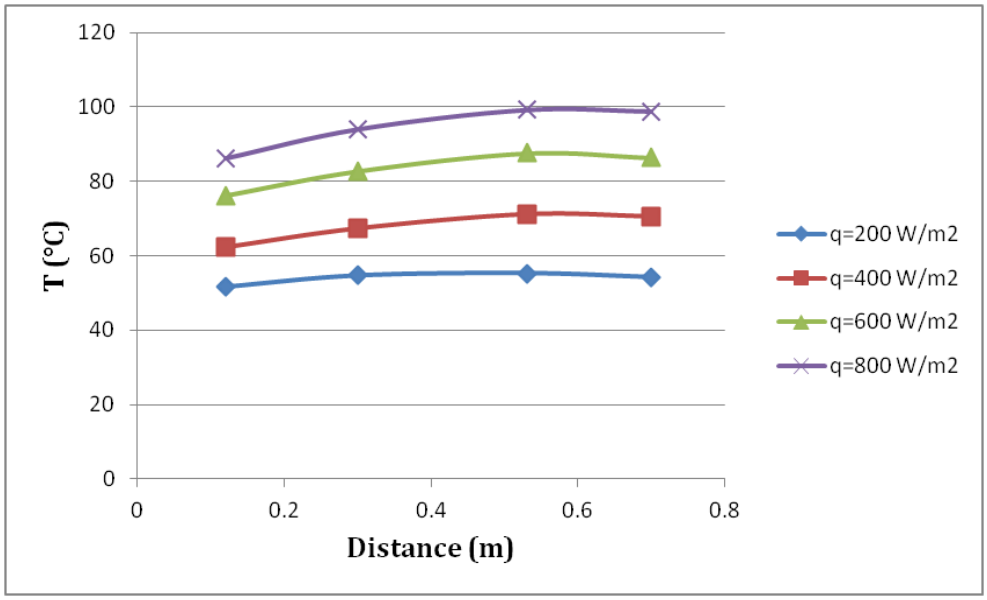

Figure 6. Variation of temperature over the length of an absorber plate for air flow (0.0019 kg/s)

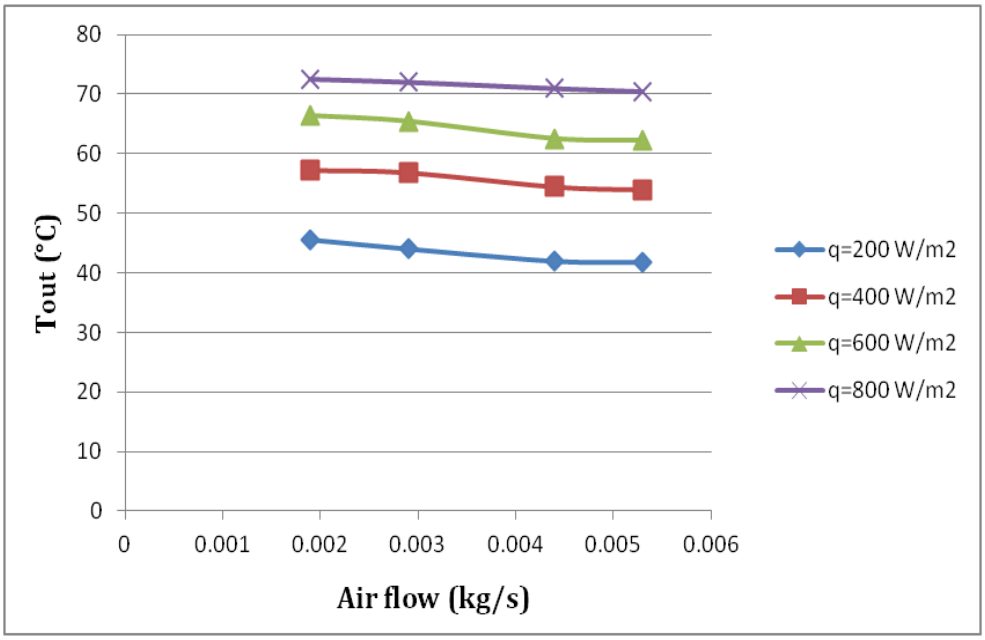

Figure 7. Variation of air outlet temperature with air flow at different values of irradiance

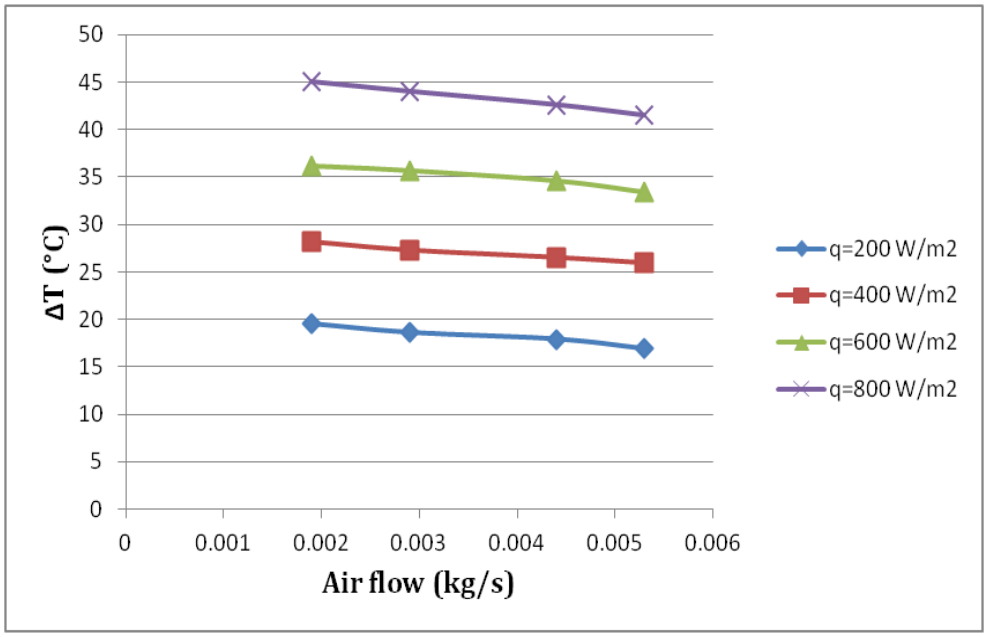

Figure 8. Experimental variation of air temperature difference with air flow at different values of irradiance

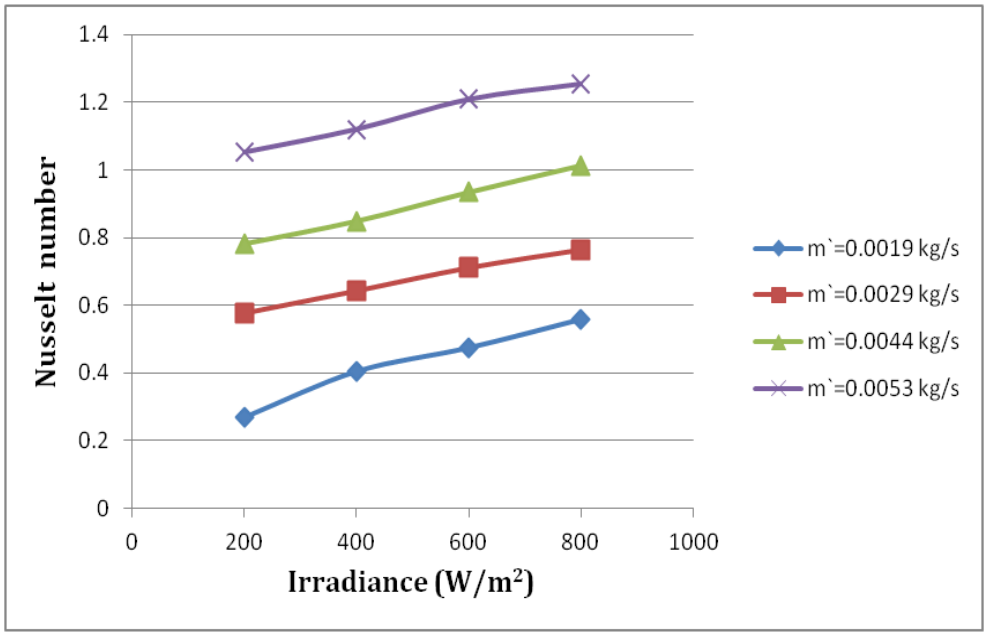

Figure 9. Variation of Nusselt number with irradiance at different values of air flow

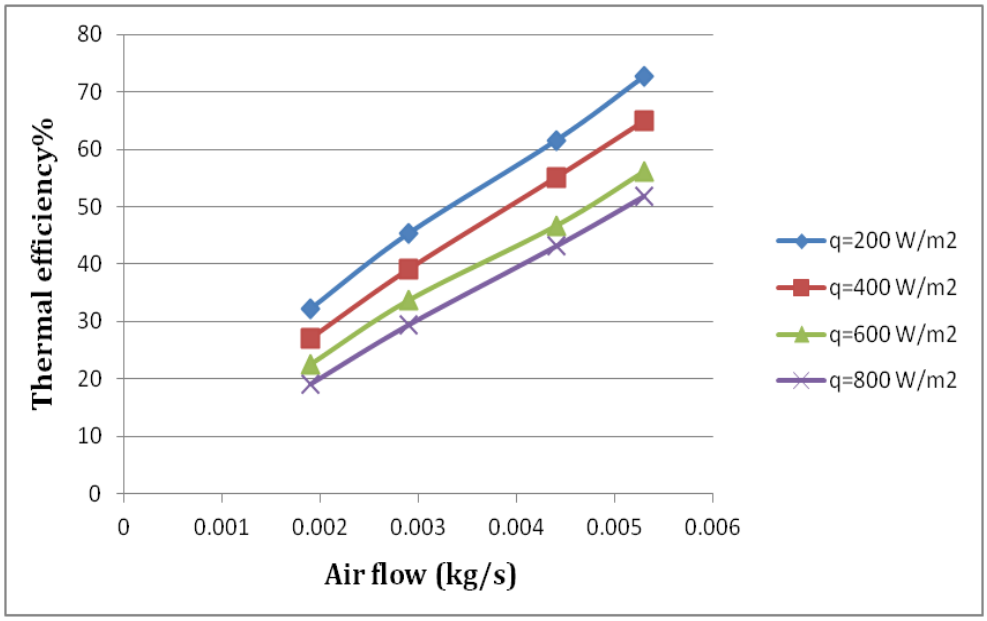

Figure 10. Experimental variation of thermal efficiency with airflow at different values of irradiance

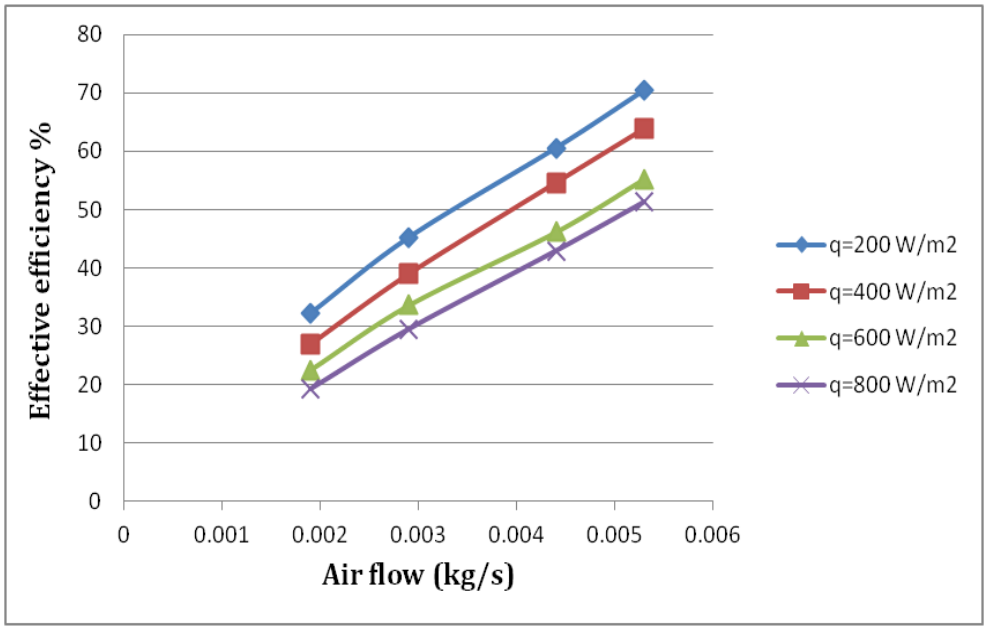

Figure 11. Experimental variation of effective efficiency with airflow at different values of irradiance

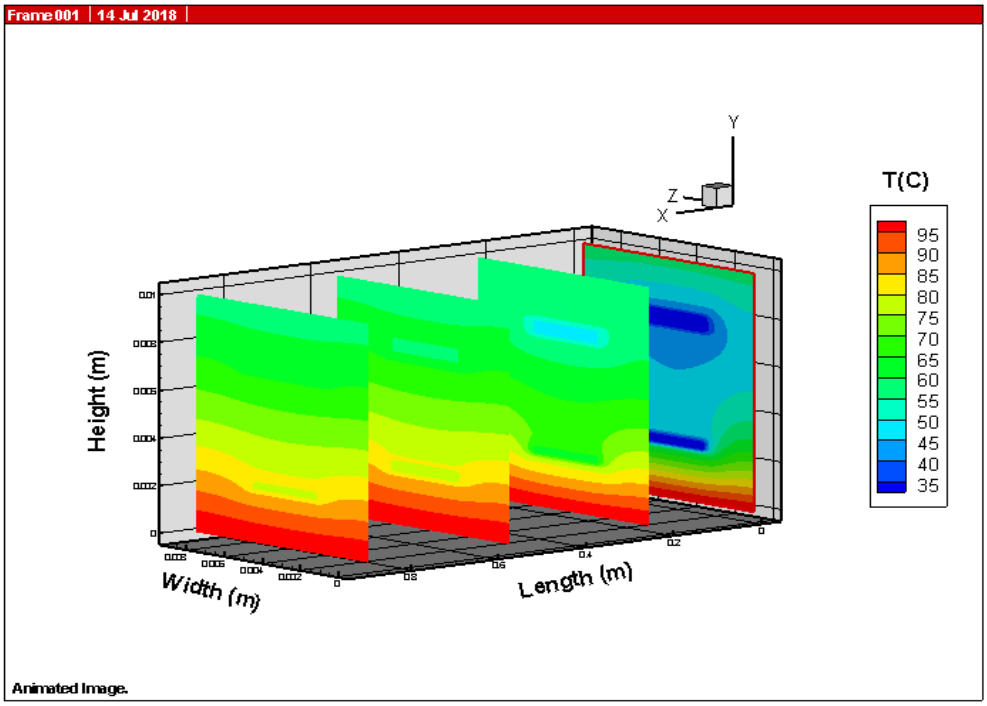

Figure 12. Isotherm contours of the plate at an irradiance of 800 W/m² and air flow of 0.0019 kg/s

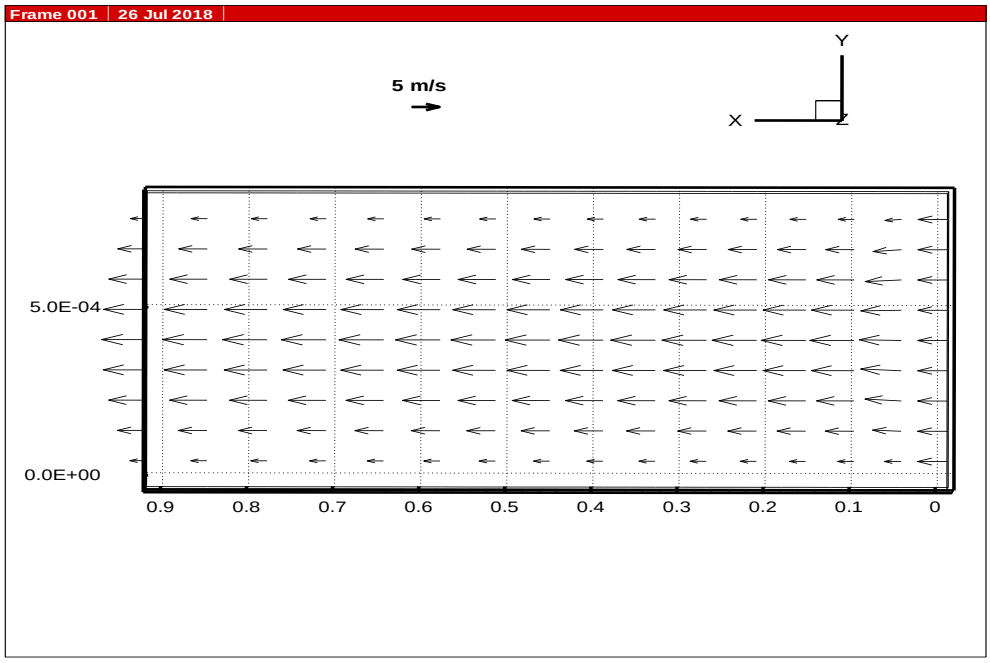

Figure 13. The flow field in micro-channel 2D, at air flow

5. Conclusions

The conclusions that can be drawn from the present study are:

1- The performance of solar collector has been improved by using the micro-channel technique that gains the highest thermal and effective efficiency of 72.8% and 70.44 %, respectively.

2- Good agreement about (3-4%) is establish when compared between experimental and the numerical results for absorber plate, mean air and outlet temperature.

3- The value of heat transfer coefficient was low, reached of 24.7 W/m² K, due to the length of the collector is high.

4- Electric control is very important to control the temperature of air out from the solar collector by the blower fan, to find the required velocity for air temperature to stay in allowable limits.
5- CFD is an important tool to analyze and type to prediction the temperature and velocity distribution in the flow of the microchannel and also to predict the temperature of the body of the microchannel.

References

[1] G. Gamrat, M. Favre-Marinet, and D. Asendrych, 2005 "Conduction and entrance effects on laminar liquid flow and heat transfer in rectangular microchannels," *International Journal of Heat and Mass Transfer*, vol. **48**, pp. 2943-2954.
[2] G. Hetsroni, A. Mosyak, E. Pogrebnyak & L. P. Yarin, 2005 "Fluid flow in micro-channels," *International Journal of Heat and Mass Transfer*, vol. **48**, pp. 1982-1998.
[3] H. Al-Bakhit and A. Fakheri, 2006 "Numerical simulation of heat transfer in simultaneously developing flows in parallel rectangular ducts," *Applied thermal engineering*, vol. **26**, pp. 596-603.
[4] P. Allen, 2007 "*Experimental and Numerical Investigation of Fluid Flow and Heat Transfer in Microchannels*," Msc Thesis, Mechanical Engineering Department, Louisiana State University.
[5] R. Sabbah, M. M. Farid, and S. Al-Hallaj, 2009 "Micro-channel heat sink with slurry of water with micro-encapsulated phase change material: 3D-numerical study," *Applied Thermal Engineering*, vol. **29**, pp. 445-454.
[6] S. S. Bertsch, E. A. Groll, and S. V. Garimella, 2009 "A composite heat transfer correlation for saturated flow boiling in small channels," *International Journal of Heat and Mass Transfer*, vol. **52**, pp. 2110-2118.
[7] L. Biswal, S. Chakraborty, and S. Som, 2009 "Design and optimization of single-phase liquid cooled microchannel heat sink," *IEEE transactions on components and packaging technologies*, vol. **32**, pp. 876-886.
[8] G. Agarwal, M. K. Moharana, and S. Khandekar, 2010 "Thermo-hydrodynamics of developing flow in a rectangular mini-channel array," *in Conference Thermo-hydrodynamics of developing flow in a rectangular mini-channel array*, pp. 1342-9.
[9] H. Mohammed, P. Gunnasegaran, and N. Shuaib, 2011 "Numerical simulation of heat transfer enhancement in wavy microchannel heat sink," *International Communications in Heat and Mass Transfer*, vol. **38**, pp. 63-68.
[10] M. K. Mansour. 2013 "Thermal analysis of novel minichannel- based solar flat-plate collector." *Energy* **60**, pp. 333-343.
[11] M. M. Mohamed and M. A. A. El-Baky, 2013 "Air Cooling of Mini-Channel Heat Sink in Electronic Devices," *Journal of Electronics Cooling and Thermal Control*, vol. **3**, pp. 49.
[12] M. A. Amraoui and K. Aliane, 2014 " Numerical Analysis of a Three-Dimensional Fluid Flow in a Flat Plate Solar Collector", *International Journal of Renewable and Sustainable Energy*. **3**(3), pp. 68-75.
[13] L. Xia and Y. Chan, 2015 "Investigation of the enhancement effect of heat transfer using micro channel," *Energy Procedia*, vol. **75**, pp. 912-918.
[14] Z. Jiandong, T. Hanzhong, and C. Susu. 2015 "Numerical simulation for structural parameters of flat-plate solar collector." *Solar Energy* **117**, pp. 192-202,.
[15] C. Sun, Y. Liu, C. Duan, Y. Zheng, H. Chang and S. Shu 2016 "A mathematical model to investigate on the thermal performance of a flat plate solar air collector and its experimental verification" *Energy Conversion and Management* **115**, pp. 43-51.
[16] M. T. Al-Asadi, F. Alkasmoul, and M. Wilson, 2016 "Heat transfer enhancement in a micro-channel cooling system using cylindrical vortex generators," *International Communications in Heat and Mass Transfer*, vol. **74**, pp. 40-47.
[17] A. A. Abdulrasool, E. M. Fayyadh, and A. A. Mohammed, 2017 "Prediction of two-phase flow boiling characterestics in microchannels heat sink by artificial neural network" *Journal of Engineering and Sustainable Development*, Vol. **21**.

[18] Y. Liu, W. Sun, and S. Wang, 2017 "Experimental investigation of two-phase slug flow distribution in horizontal multi-parallel micro-channels," *Chemical Engineering Science*, Vol. **158**, pp. 267-276.
[19] B. Kwon, N. I. Maniscalco, A. M. Jacobi, and W. P. King, 2018 "High power density air-cooled microchannel heat exchanger," *International Journal of Heat and Mass Transfer*, Vol. **118**, pp. 1276-1283.
[20] S. Rai, P. Chand, and S. P. Sharma. 2018 "Evaluation of thermo hydraulic effect on offset finned absorber solar air heater." *Renewable Energy* **125**, pp. 39-54.